

Title	Cationic Copolymerization of Styrene Derivatives and Oxiranes via Concurrent Vinyl-Addition and Ring-Opening Mechanisms: Multiblock Copolymer Formation via Occasional Crossover Reactions
Author(s)	Kanazawa, Arihiro; Aoshima, Sadahito
Citation	Macromolecules. 2020, 53(13), p. 5255-5265
Version Type	AM
URL	https://hdl.handle.net/11094/100932
rights	This document is the Accepted Manuscript version of a Published Work that appeared in final form in Macromolecules, © American Chemical Society after peer review and technical editing by the publisher. To access the final edited and published work see https://doi.org/10.1021/acs.macromol.0c00854
Note	

The University of Osaka Institutional Knowledge Archive : OUKA

<https://ir.library.osaka-u.ac.jp/>

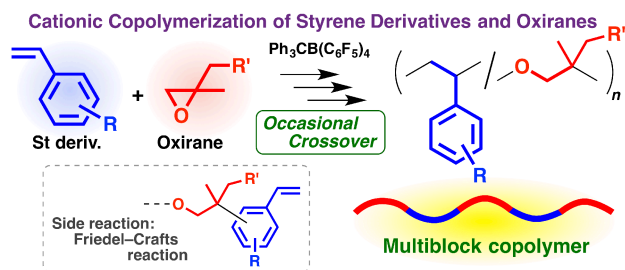
The University of Osaka

Cationic Copolymerization of Styrene Derivatives and Oxiranes via Concurrent Vinyl-Addition and Ring-Opening Mechanisms: Multiblock Copolymer Formation via Occasional Crossover Reactions

Arihiro Kanazawa and Sadahito Aoshima**

Department of Macromolecular Science, Graduate School of Science, Osaka University, Toyonaka,
Osaka, 560-0043, Japan

For TOC use only:



Abstract

Styrene derivatives were demonstrated to cationically copolymerize with 2,2-disubstituted oxiranes, which can generate a tertiary carbocation by the ring opening of the oxonium ion, through crossover reactions. The copolymerization proceeded with comparable consumptions of both the vinyl and cyclic monomers when appropriate combinations, such as *p*-methoxystyrene and 2-ethylhexyl β -methylglycidyl ether or *p*-methylstyrene and β -methylepiclorohydrin, in terms of reactivity were used. The homopropagation reactions of both monomers occur preferentially compared to the crossover reactions, which resulted in multiblock copolymers with relatively long blocks. The oxirane-derived carbocation caused both Friedel–Crafts reactions with a styrene derivative and β -proton elimination as chain transfer reactions. For the analysis of the copolymer structures, unlike the acetal structure resulting from the crossover from a vinyl ether to an oxirane, the *sec*-benzylic ether structure derived from the crossover from a styrene derivative to an oxirane was difficult to detect by ^1H NMR

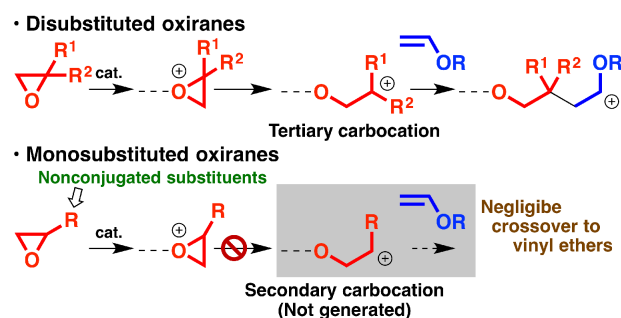
spectroscopy due to overlap with the peaks of the oxirane units in the main chain. However, the occurrence of crossover reactions was confirmed by ^{13}C NMR analysis by comparison with the spectra of model polymers. Acidolysis of the *sec*-benzylic ether structure by trifluoroacetic acid also facilitated the determination of the copolymer structure.

Introduction

Copolymerizations of different types of monomers have attracted increasing interest because generally incompatible monomers can be incorporated into a single polymer chain. A simple and easily accessible method to create such copolymers is the use of a bifunctional initiator that has initiating sites for different polymerization reactions.^{1–4} Unlike copolymerizations via orthogonal propagation reactions at different propagating ends, however, copolymerizations via a common intermediate or through interconversion of the propagating species via crossover reactions at a single propagating end have great potential to generate copolymers that are otherwise difficult to obtain.^{5–17} For example, interconvertible living radical and cationic polymerization employing a common intermediate successfully afforded copolymers consisting of cationically and radically polymerizable monomers such as vinyl ethers (VEs) and acrylates.^{5,6} Copolymerizations of vinyl and cyclic monomers generate copolymers through the interconversion of the propagating species via crossover reactions,^{7–16} although in most cases, such copolymerizations are difficult due to the large difference in reactivities of both monomers and the propagating species.

Both VEs and oxiranes undergo cationic polymerization; however, it is generally difficult to copolymerize these monomers via crossover reactions because they polymerize via different types of propagating species. In particular, a primary reason that their crossover is difficult is that the oxonium ion generated from the oxirane monomer does not react with the vinyl monomer. In recent years, however, we developed a cationic copolymerization of VEs and oxiranes via concurrent vinyl addition and ring-opening mechanisms through the design of monomer structures and initiating systems.^{14–16} To overcome the anticipated drawbacks, we used oxiranes with two alkyl groups at the 2-position of the oxirane ring, such as isobutylene oxide and β -methylglycidyl ethers (β MGEs), because the oxonium ion derived from those oxiranes can potentially undergo a ring-opening reaction to generate a tertiary carbocation, which is more stable than the secondary carbocation that would be generated from a

monosubstituted oxirane (Scheme 1). The copolymerization of such oxiranes with alkyl VEs successfully proceeded via crossover reactions and yielded a copolymer with a multiblock sequence. Oxiranes that generate resonance-stabilized, allyl-type carbocations by ring opening, such as isoprene monoxide and butadiene monoxide, were also suitable monomers for this copolymerization. In addition, the use of a catalyst or an initiator, such as $B(C_6F_5)_3$ or $Ph_3CB(C_6F_5)_4$, that generates a weakly coordinating counteranion was indispensable for the generation of the cationic propagating species from both VEs and oxiranes. Indeed, the copolymerization did not proceed efficiently when metal chlorides such as $GaCl_3$ were used because the carbon–chlorine bond that was generated at the oxirane-derived propagating end by the reaction with the metal chloride-derived chloride anion was inert and could not be cleaved to generate a carbocation.

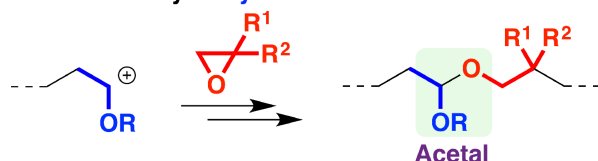


Scheme 1. Crossover reactions from oxiranes to vinyl ethers.

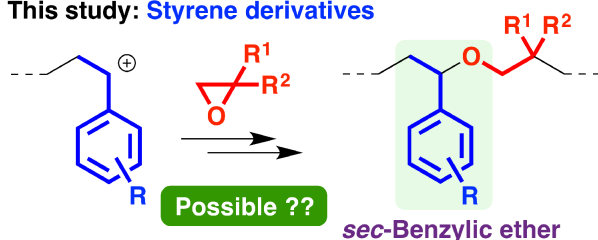
Styrene (St) derivatives are promising monomers that can potentially copolymerize with oxiranes via a cationic pathway. St derivatives generally exhibit lower reactivities than alkyl VEs, although the substituents on the aryl ring greatly affect the reactivity. In addition, an acetal structure is generated as a result of the crossover from a VE to an oxirane,^{14–16} while the structure resulting from the crossover from a St derivative to an oxirane is a *sec*-benzylic ether (Scheme 2). Moreover, the propagating carbocations derived from VE and the St derivative are adjacent to an alkoxy group or an aryl ring, respectively. Therefore, these differences in the reactivity, the resulting structures, and the propagating carbocations can potentially affect the occurrence and frequency of the crossover reactions in the copolymerization with oxiranes. Indeed, an oxirane ring was more prone to react with a VE-derived carbocation than a St derivative-derived carbocation in the cationic polymerization of a VE or a St derivative bearing an oxirane moiety as a side chain.^{18,19} Studies on the copolymerization of St

and oxiranes were reported in the 1960s; however, it was unclear whether crossover reactions occurred because the products were analyzed only by elemental analysis, infrared spectroscopy, and fractional extraction.^{20,21} In particular, a copolymer was suggested to be produced not via crossover reactions but by chain transfer reactions in the copolymerization of St and epichlorohydrin.²¹ Detailed analysis of copolymerization products by NMR spectroscopy is indispensable for confirming copolymerization via crossover reactions.

• Previous study: Vinyl ethers



• This study: Styrene derivatives



Scheme 2. Crossover reactions from vinyl monomers to oxiranes.

In this study, we examined the cationic copolymerization of St derivatives and oxiranes with a focus on elucidating the structures of the products. In particular, we aimed to detect the occurrence of crossover reactions between the different types of monomers. When St derivatives and oxiranes with appropriate reactivities were combined, both monomers were consumed during the polymerization. Subsequently, the occurrence of crossover reactions was demonstrated through NMR analysis of the copolymerization products, acidolysis products, and model polymers. The copolymerization proceeded via preferential homopropagation and occasional crossover reactions, resulting in the generation of multiblock copolymers with several blocks per chain. Friedel–Crafts reactions on the aryl rings also occurred as a side reaction and are characteristic of St derivatives.

Experimental Section

Materials. *p*-Methoxystyrene (pMOS; Wako, >97.0%) was dried overnight over sodium sulfate and

then distilled twice over calcium hydride under reduced pressure. *p*-Methylstyrene (pMeSt; TCI, >96.0%), St (Wako, >99%), and 2,4,6-trimethylstyrene (triMeSt; Sigma-Aldrich, 95%) were washed a 10% aqueous sodium hydroxide solution and then with water, dried overnight over sodium sulfate, and distilled twice over calcium hydride under reduced pressure. β -Methylepiclorohydrin [MECH; Chemexcel (Zhangjiakou) Fine Chemicals: kindly supplied by ADEKA Corporation] was distilled twice over calcium hydride under reduced pressure. Isobutylene oxide (IBO; TCI, >97.0%) was distilled twice over calcium hydride. 2-Ethylhexyl β MGE (EHMGE) and phenyl β MGE (PMGE), which were synthesized by the reaction of MECH with 2-ethylhexanol and phenol, respectively, and then distilled twice over calcium hydride as reported in a previous study,¹⁶ were kindly supplied by ADEKA Corporation. Triphenylmethylium tetrakis(pentafluorophenyl)borate [$\text{Ph}_3\text{CB}(\text{C}_6\text{F}_5)_4$; TCI, >98.0%], SnCl_4 (Sigma-Aldrich, 1.0 M solution in heptane), ethanesulfonic acid (Sigma-Aldrich, 95%), and tetrabutylammonium chloride ($n\text{Bu}_4\text{NCl}$; Fluka, $\geq 99.0\%$) were used as received. Dichloromethane (Wako, super dehydrated) and hexane (Wako, 96.0%) were dried by passage through a solvent purification column (Glass Contour).

Polymerization procedures. The following is the typical polymerization procedure. A glass tube equipped with a three-way stopcock was dried using a heat gun (Ishizaki, PJ-206A; the air temperature was approximately 450 °C) under dry nitrogen. Dichloromethane, hexane (internal standard for gas chromatography), pMeSt, and MECH were sequentially added into the tube using dry syringes. The polymerization was started by the addition of a prechilled solution of $\text{Ph}_3\text{CB}(\text{C}_6\text{F}_5)_4$ in dichloromethane to the monomer solution at -40 °C. After a predetermined time, the reaction was terminated by the addition of methanol containing a small amount of aqueous ammonia. The quenched mixture was diluted with dichloromethane and hexane and then washed with an aqueous sodium hydroxide solution and then with water. The volatiles were then removed under reduced pressure. The monomer conversion was determined by gas chromatography (column packing material: PEG-20M-Uniport HP; GL Sciences Inc.) using hexane as an internal standard or by a combination of gravimetry and ^1H NMR analysis of the product.

Acidolysis. Acidolysis of the copolymers and the model polymer was conducted with 0.5 M trifluoroacetic acid in dichloromethane (sample: approximately 2 wt%) at room temperature for 1 h. The quenched mixture was washed with an aqueous sodium hydroxide solution and then water. The volatiles were removed by evaporation to yield a product.

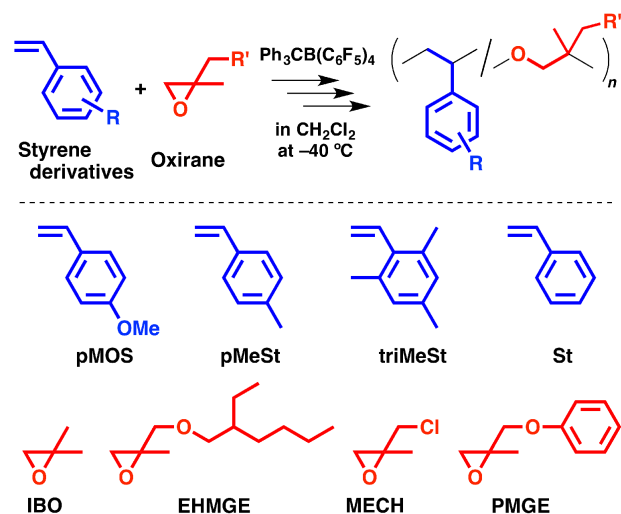
Transformation of the carbon–chlorine bond at the chain end of poly(pMeSt) into the carbon–alkoxy bond.²² First, a poly(pMeSt) with a chlorine atom at the chain end was prepared by the living cationic polymerization of pMeSt with ethanesulfonic acid/SnCl₄/*n*Bu₄NCl as the initiating system.²³ After purification by reprecipitation from methanol, poly(pMeSt) was dissolved in dichloromethane. To the solution were sequentially added 2-methoxyethanol or methanol and a silver hexafluorophosphate solution in dichloromethane. Soon after the addition of the silver salt, a white precipitate (AgCl) was formed. The reaction mixture was left overnight at room temperature, and it was then washed with water and purified by reprecipitation from methanol.

Characterization. The molecular weight distribution (MWD) of the polymers was measured by gel permeation chromatography (GPC) in chloroform at 40 °C with polystyrene gel columns [TSKgel GMH_{HR}-M × 2 (exclusion limit molecular weight (MW) = 4×10^6 ; bead size = 5 μm; column size = 7.8 mm id × 300 mm); flow rate = 1.0 mL/min] connected to a Tosoh DP-8020 pump, a CO-8020 column oven, a UV-8020 ultraviolet detector, and an RI-8020 refractive-index detector. The number-average molecular weight (M_n) and polydispersity ratio [weight-average molecular weight/number-average molecular weight (M_w/M_n)] were calculated from the chromatograms with respect to 16 polystyrene standards (Tosoh; MW = 5.0×10^2 to 1.09×10^6 , $M_w/M_n < 1.2$). The absolute M_n values were determined with a GPC system comprising of a Viscotek VE 1122 pump, polystyrene gel columns (TSKgel GMH_{HR}-M × 2; flow rate = 0.7 mL/min; eluent: tetrahydrofuran), and a Viscotek TDA 305 triple detector [refractive index, laser light scattering ($\lambda = 670$ nm; 90 ° RALS and 7 ° LALS), and differential pressure viscometer]. The purification of the polymerization products by preparative GPC was conducted in chloroform at room temperature with a polystyrene gel column [TSKgel G3000H_{HR} (exclusion limit MW = 6×10^4 ; bead size = 5 μm; column size = 21.5 mm id × 300 mm); flow rate = 2.0 mL/min] connected to a JASCO PU-2086 Plus pump, a JASCO UV-2075 ultraviolet detector, and a Tosoh RI-8020 refractive-index detector. The NMR spectra were recorded using a JEOL JNM-ECA 500 spectrometer (500.16 MHz for ¹H, 125.77 MHz for ¹³C, and 470.62 MHz for ¹⁹F) or a JEOL JNM-ECS 400 spectrometer (399.78 MHz for ¹H and 100.53 MHz for ¹³C) in chloroform-*d* at 30 °C.

Results and Discussion

Cationic Copolymerization of Styrene Derivatives and Oxiranes

The St derivative and oxirane need to exhibit comparable reactivities for them to be simultaneously consumed in the polymerization. To examine appropriate combinations of monomers, we employed two St derivatives and three oxiranes with different substituents in the cationic copolymerization using $\text{Ph}_3\text{CB}(\text{C}_6\text{F}_5)_4$, which is an effective initiator for the copolymerization of VEs and oxiranes,¹⁶ in dichloromethane at $-40\text{ }^\circ\text{C}$ (Scheme 3). pMOS exhibits a higher reactivity than pMeSt due to the electron-donating resonance effect of the methoxy group on the aromatic ring. The reactivity of the oxiranes decrease in the order of $\text{IBO} > \text{EHMGE} > \text{MECH}$ due to the electron-withdrawing effects of the alkoxy group and the chlorine atom of EHMGE and MECH, respectively.¹⁶ These oxiranes all have two substituents at the 2-position and can thus potentially generate tertiary carbocations via the ring opening of the oxonium ions. Monosubstituted oxiranes such as alkyl glycidyl ethers and monoalkyloxiranes are most likely inefficient for the copolymerization because unstable secondary carbocations are negligibly generated via the ring opening (Scheme 1), as reported in previous studies of the copolymerization with VEs.^{15,16}



Scheme 3. Cationic copolymerization of styrene derivatives and oxiranes.

Based on a series of copolymerization reactions (Table 1), the St derivative and oxirane were consumed at comparable rates when monomers with appropriate reactivities were used. In the case of pMOS, the copolymerization with EHMGE (entry 2) proceeded more efficiently than the reactions with the other two oxiranes (entries 1 and 4). A polymer with an M_n value of approximately five thousand was obtained, although small peaks likely attributable to EHMGE oligomers were observed in the

lower MW region of the MWD curve (Figure 1A). The ^1H NMR spectrum of the high-MW fraction obtained from preparative GPC (broken curve in Figure 1A) had peaks assignable to both pMOS and EHMGE units (Figure S3A). The ratio of EHMGE units in the higher-MW fraction was lower than the original product, which also indicates that oligomers mainly consisting of EHMGE were most likely generated in the copolymerization (“S/O ratio” column in Table 1). In contrast, only a small amount of pMOS was consumed in the copolymerization with IBO (entry 1), a more reactive oxirane than EHMGE, to give a low MW product with an M_n of 1.4×10^3 . ^1H NMR analysis suggested that a very small amount of pMOS was incorporated into the product (Figure S2A; the mole fraction of pMOS was approximately 0.12). When MECH, a less reactive oxirane than EHMGE, was used, pMOS was exclusively consumed, yielding a pMOS homopolymer with a very high MW (entry 4; Figure S5A).

Table 1. Cationic Copolymerization of Styrene Derivatives and Oxiranes^a

Entry	St derivatives (M)	Oxirane (M)	Time	St derivatives		$M_n \times 10^{-3}^d$	M_w/M_n^d	S/O ratio (mol%) ^e	After acidolysis ^f		
				ves cony (%) ^b	cony (%) ^b				$M_n \times 10^{-3}^d$	M_w/M_n^d	S/O ratio (mol%) ^e
1	pMOS (0.75)	IBO (0.75)	10 min	6 ^h	46 ^h	1.4	1.82	12/88	–	–	–
2	pMOS (0.76)	EHMGE (0.76)	0.5 h	21	40	5.2 ^h [5.5]	1.50 ^h [1.47]	39/61 [61/39]	2.3	1.80	63/37
3	pMeSt (0.76)	EHMGE (0.76)	2 h	<1 ^g	17 ^g	1.0	1.66	3/97	–	–	–
4	pMOS (0.75)	MECH (0.76)	5 s	99	0	>450 ⁱ	>1.6 ⁱ	100/0	–	–	–
5	pMeSt (0.76)	MECH (0.76)	3 h	90	81	5.0 [6.4]	1.90 [1.62]	54/46 [61/39]	2.3	2.14	63/37
6	pMeSt (0.76)	MECH (1.5)	1.5 h	70	78	3.4 [4.1]	1.79 [1.62]	31/69 [34/66]	1.3	2.09	38/62
7 ^g	pMeSt (0.76)	MECH (0.77)	3 h	13	64	0.5	1.94	–	–	–	–
8	triMeSt (0.76)	MECH (0.76)	2 h	56	74	4.4 [4.7]	2.10 [1.97]	41/59 [49/51]	2.3	2.90	52/48
9	St (0.76)	MECH (0.75)	7 h	15	80	1.4	1.67	12/88	–	–	–
10	pMeSt (0.76)	PMGE (0.75)	2.2 h	9	74	1.5	1.86	18/82	–	–	–
11	pMOS (0.75)	–	10 s	98	–	>580 ⁱ	>2.3 ⁱ	–	–	–	–
12	pMeSt (0.76)	–	1 min	100	–	>34 ⁱ	>9.7 ⁱ	–	–	–	–
13	–	MECH (0.76)	24 h	–	52	2.3 [3.3]	1.73 [1.48]	–	0.8	1.76	–

^a $[\text{Ph}_3\text{CB}(\text{C}_6\text{F}_5)_4]_0 = 3.0 \text{ mM}$, in dichloromethane at -40°C . See Figures 1 and S1 for the MWD curves. See Figures 2, S2–S16, and S21–S28 for the NMR spectra. ^b By gas chromatography. ^c Values in parenthesis were measured after purification by preparative GPC. ^d By GPC (polystyrene calibration). ^e The molar ratio of St derivative/oxirane in the product. By ^1H NMR. ^f Acidolysis was conducted after purification by preparative GPC. ^g In toluene. ^h By the combination of gravimetry and ^1H NMR analysis of the product. ⁱ A part of polymer chains exceeded the exclusion-limit MW of the GPC columns.

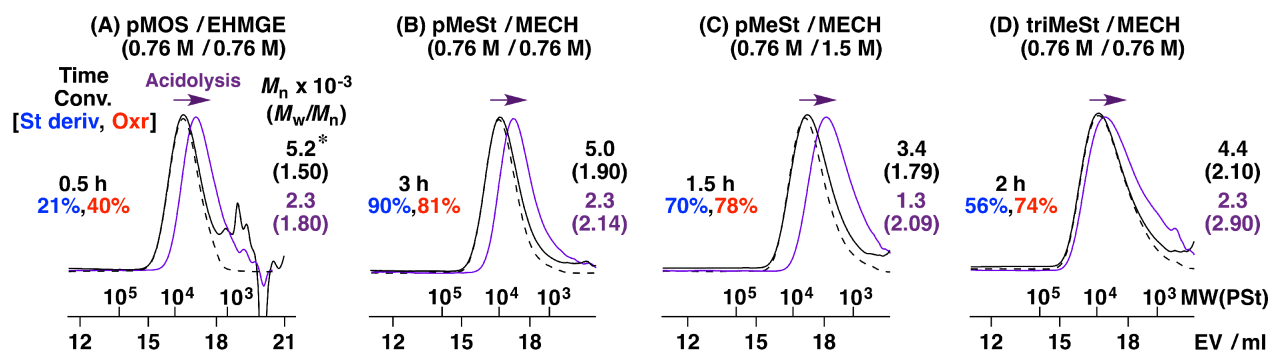


Figure 1. MWD curves of the copolymerization products of (A) pMOS and EHMGE (entry 2 in Table 1; * values for a main peak); (B), (C) pMeSt and MECH (entries 5 and 6); and (D) triMeSt and MECH (entry 8) (see the footnote of Table 1 for the reaction conditions) [solid line (black): original product, broken line: after purification by preparative GPC, purple line: acidolysis product (acidolyzed after purification by preparative GPC)].

Unlike the case of pMOS, MECH was most appropriate for copolymerization with pMeSt among the three oxiranes. Both pMeSt and MECH were consumed in the copolymerization, yielding a polymer with an M_n of five thousand (entry 5).²⁴ A polymer with a lower MW was obtained when the concentration of MECH was doubled (entry 6), which suggests that the MW depends on the chain transfer reactions at the oxirane-derived propagating ends. Indeed, a lower MW product was obtained in the homopolymerization of MECH under the same conditions (entry 13), while a very high-MW polymer was produced in the homopolymerization of pMeSt (entry 12). A detailed analysis of the polymer structure by a series of NMR measurements is described in the next section. When EHMGE was used instead of MECH, negligible pMeSt was consumed, resulting in the generation of EHMGE oligomers (entry 3; Figure S6).

Polymerization rates likely depended on the reactivity of oxiranes. The homopolymerizations of pMOS (entry 11 in Table 1) and pMeSt (entry 12) proceeded very fast, while the consumption rates of pMOS and pMeSt were much smaller in the copolymerizations with EHMGE (entry 2) and MECH (entries 5 and 6), respectively. In addition, pMOS, which is a more reactive St derivative than pMeSt, was consumed very fast in the presence of MECH and MECH was not consumed at all (entry 4). These results probably indicate that the reactivity of St derivatives-derived propagating species are suppressed via the interaction with an oxirane monomer with an appropriate reactivity and that the propagation reactions of oxiranes are relatively slow and function as a rate-determining step in the

copolymerization.

NMR Analysis of the Copolymerization Products: Assignments of the Structures Resulting from Crossover Reactions

To investigate whether crossover reactions occurred between the St derivatives and oxiranes, the products obtained from the copolymerization of pMeSt and MECH were analyzed by ^1H , ^{13}C , DEPT 135, and 2D (^1H – ^1H COSY, ^1H – ^{13}C HSQC, and ^1H – ^{13}C HMBC) NMR measurements (Figures 2, 3, and S7–S11). First, we tried to detect the *sec*-benzylic ether structure, which is generated as a result of the crossover reaction from a St derivative to an oxirane (Scheme 4A). To determine the chemical shift of this structure, a poly(pMeSt) with an alkoxy group at the chain end was prepared as a model polymer via a literature method employing the reaction of a chlorine-capped poly(pMeSt) with a silver salt and an alcohol.²² pMeSt homopolymers with 2-methoxyethoxy and methoxy groups, which were prepared using 2-methoxyethanol and methanol, had peaks assignable to methine protons at 3.6–3.8 and 3.5–3.7, respectively (Figures 2E and S17; Table 2). In the spectrum of the copolymerization product of pMeSt and MECH (Figure 2A), however, the large peaks of the main chain protons are in this region (shown as peak 13); hence, it was difficult to confirm the crossover-derived *sec*-benzylic ether structure by ^1H NMR spectroscopy. This is in sharp contrast to the easy assignment of the acetal structures derived from the crossover from VE to oxirane in previous studies.^{14–16}

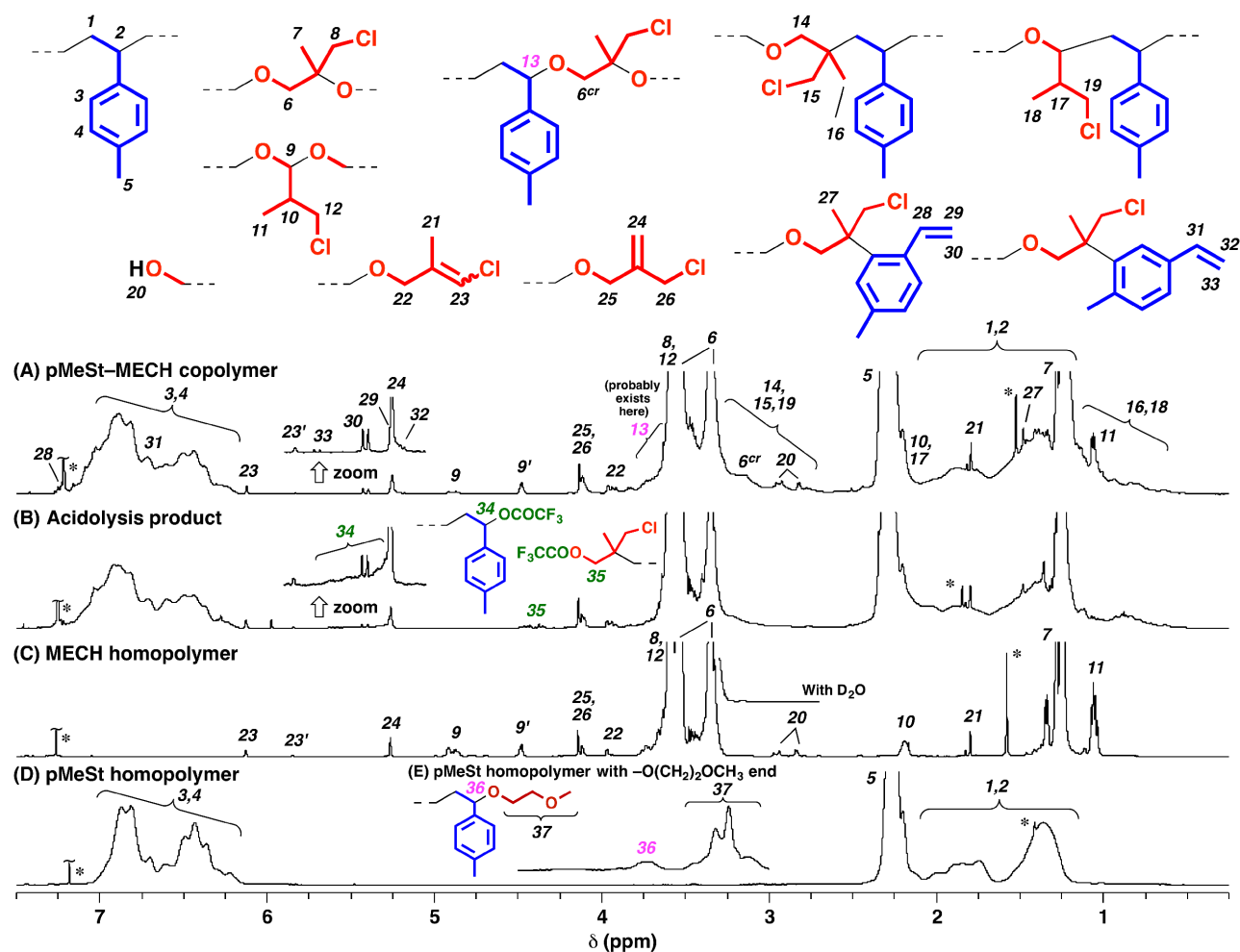
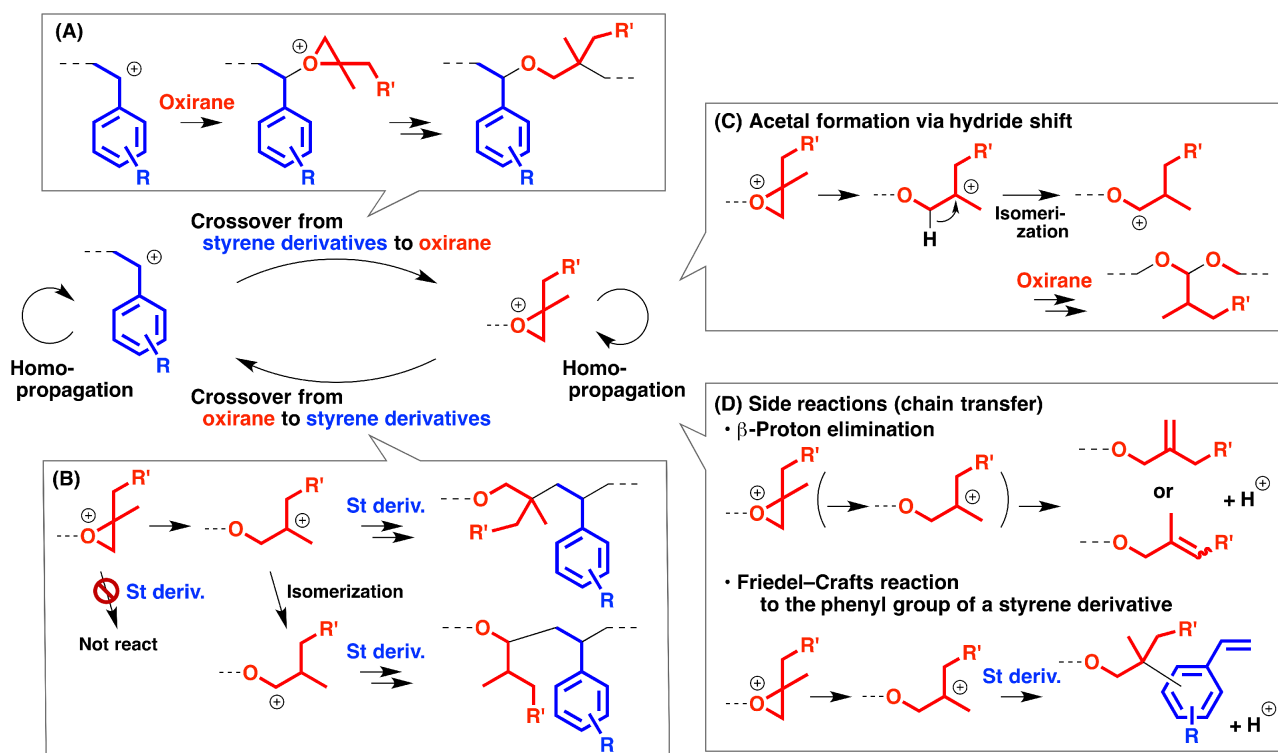


Figure 2. ^1H NMR spectra of (A) the copolymerization product of pMeSt and MECH (entry 6 in Table 1; after purification by preparative GPC; broken curve in Figure 1C; see also ^{13}C and 2D NMR spectra in Figures S7–S11), (B) its acidolysis product (purple curve in Figure 1C), (C) MECH homopolymer (entry 13; after purification by preparative GPC; broken curve in Figure S11; see also ^{13}C and 2D NMR spectra in Figures S7 and S14–S16), (D) pMeSt homopolymer (entry 12; after purification by reprecipitation from methanol), and (E) poly(pMeSt) with an $-\text{O}(\text{CH}_2)_2\text{OCH}_3$ end (see Scheme S1 and Figure S17C). * Water and CHCl_3 .



Scheme 4. Propagation reactions and side reactions in the copolymerization of styrene derivatives and oxiranes.

Table 2. ^1H and ^{13}C NMR chemical shifts (ppm) of the methine protons and carbons at the polymer chain end and monomeric compounds^a

	Polymer chain end		Monomeric	
X	^1H	^{13}C	^1H (R)	^{13}C (R)
$-\text{O}(\text{CH}_2)_2\text{OCH}_3$	3.6–3.8	79–81	4.3 (H) ^b	–
$-\text{OCH}_3$	3.5–3.7	–	4.3 (Me) ^b	80 (H) ^b
$-\text{OCOCF}_3$	5.2–5.6	78–80	6.0 (H) ^b	82 (H) ^b
$-\text{Cl}$	4.3–4.5	61–62	5.1 (Me) ^b	59 (Me) ^b

^a See Figures 2, 3 S17, and S18 for the spectra of the polymers. ^b References 25–29 for the monomeric compounds.

Unlike ^1H NMR, analysis by ^{13}C NMR spectroscopy successfully revealed the presence of the motif derived from the crossover from a St derivative to an oxirane. Two peaks were observed at 79–81 ppm in the spectrum of the product obtained from the copolymerization of pMeSt and MECH

(Figure 3A; peak 13 in Figure S7A and S7C). The model pMeSt polymer with a 2-methoxyethoxy chain end exhibited similar peaks in this region (Figures 3C), while such peaks were not present in the spectra of the MECH homopolymer (Figures 3E) and the poly(pMeSt) obtained with $\text{Ph}_3\text{CB}(\text{C}_6\text{F}_5)_4$ (Figure 3F). In addition, these peaks disappeared (shifted upfield) after acidolysis, as discussed below (Figure 3B and 3D). From these results, the peaks at 79–81 ppm are assignable to the *sec*-benzylic ether structure derived from the crossover from pMeSt to MECH. A difference in steric demands of a few pMeSt units near the chain end is likely responsible for the presence of two peaks. In addition, similar peaks were observed in the spectrum of the product obtained from the copolymerization of pMOS and EHMGE (Figure S4A), which indicates that the crossover from pMOS to EHMGE also proceeded.

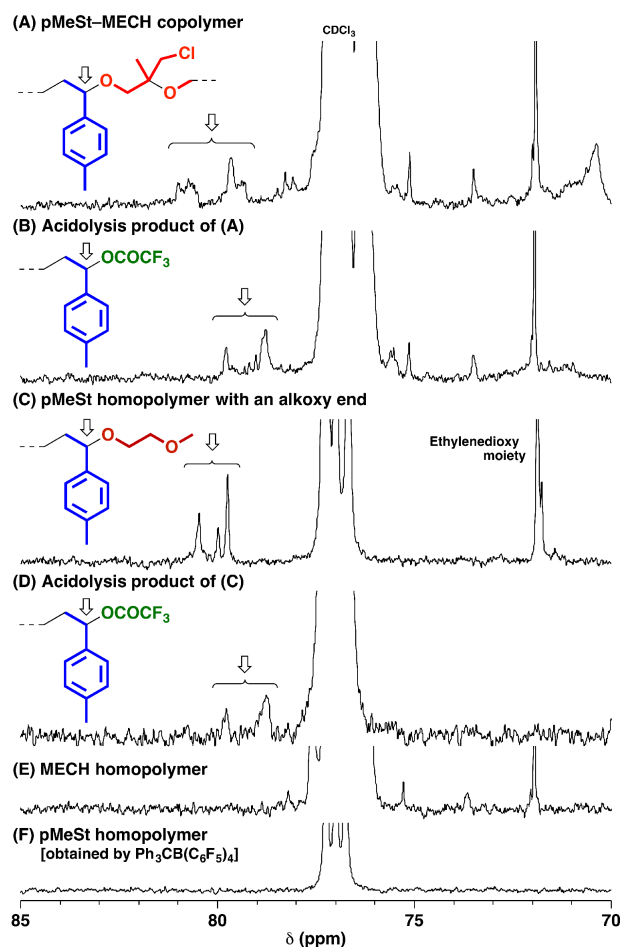


Figure 3. ^{13}C NMR spectra (70–85 ppm; see Figures S7 and S18 for the spectra at a wider region and DEPT 135 spectra) of (A) the copolymerization product of pMeSt and MECH (entry 6 in Table 1; after purification by preparative GPC; broken curve in Figure 1C), (B) its acidolysis product (after

purification by preparative GPC), (C) pMeSt homopolymer with a MeOCH₂CH₂O end (Scheme S1), (D) its acidolysis product, (E) MECH homopolymer (entry 13; after purification by preparative GPC), and (F) pMeSt homopolymer (entry 12; after purification by reprecipitation from methanol).

The structures derived from the crossover from an oxirane to a St derivative (Scheme 4B) most likely correspond to the shoulder-like peaks at approximately 3.0 and 1.0 ppm (peaks 14, 15, 19, 16, and 18 in Figure 2A). Such peaks were not observed in the spectra of the MECH and pMeSt homopolymers (Figure 2C and 2D), which suggests that structures derived from the crossover reactions are likely responsible for these peaks. MECH units adjacent to pMeSt units are also believed to exhibit peaks at these regions. The homosequence of pMeSt probably affects the chemical shifts of the protons of the neighboring structures due to the effects of the aromatic rings, causing the MECH peaks to be shifted upfield relative to those of the MECH homosequence. Indeed, the peaks of the chain end methine protons of the pMeSt homopolymers were shifted upfield by 0.4–0.8 ppm relative to those of the corresponding monomeric compounds^{25–29} (Table 2). In addition, the 2-methoxyethoxy and methoxy moieties at the poly(pMeSt) chain end exhibited peaks at a higher field (3.0–3.5 ppm and 2.9–3.1 ppm, respectively) than the peaks of the corresponding monomeric compounds (3.4 and 3.2 ppm, respectively;^{25,26} Figure S17C). Similar upfield shifts most likely occurred in the MECH units adjacent to the pMeSt units. Several correlations that are likely assignable to such structures were also observed in the ¹H–¹³C HMBC spectra (Figures S10 and S11). The spectra of the pMOS and EHMGE copolymerization products also showed shoulder-like peaks at higher fields than the corresponding peaks of the EHMGE homosequences (Figure S3A).

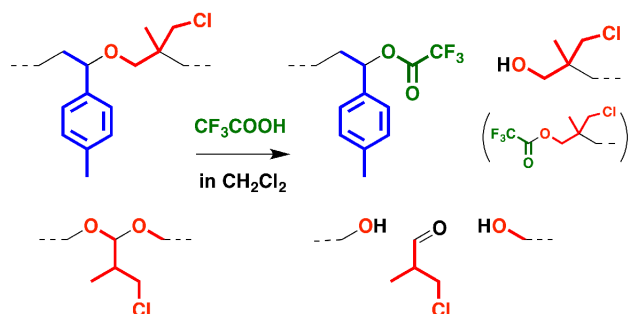
The peaks other than those assigned to the main chain and the crossover-derived structures include peaks assignable to acetal moieties resulting from the isomerization of the MECH-derived propagating carbocation and the peaks of chain ends derived from β-proton elimination reactions and the Friedel–Crafts reactions involving a St derivative monomer. The peaks at 4.5 and 4.9 ppm, which were also observed in the spectrum of the MECH homopolymer, were assigned to acetal moieties (peaks 9 and 9'). The isomerization of the MECH-derived carbocation via a hydride shift and subsequent reaction with an MECH monomer generates an acetal moiety (Scheme 4C).^{14–16} The difference in the scission mode (α- or β-scission) of the neighboring MECH units is most likely responsible for the two peaks (peaks 9 and 9') at different chemical shifts [the assignments are based

on the ^1H – ^{13}C HMBC spectra (Figures S10 and S11)]. Peaks assignable to *endo*- (peak 23) and *exo*-olefins (peak 24) resulting from β -proton elimination reactions at the MECH-derived propagating ends were also observed. In addition, peaks assignable to vinyl protons of styrenic moieties were observed [peaks 28–33; some peaks were assigned by 2D NMR (Figures S8–S11)]. The styrenic moieties were most likely incorporated into polymer chain ends through Friedel–Crafts reactions between the MECH-derived carbocations and the aromatic ring of a pMeSt monomer [Scheme 4D; correlations attributable to MECH units attached to the aryl ring were detected in the ^1H – ^{13}C HMBC spectra (Figures S10 and S11)], which is explained in more detail below.

Acidolysis of the Copolymerization Products

The occurrence of crossover reactions from the St derivative to the oxirane was further confirmed by acidolysis of the copolymerization product. The *sec*-benzylic ether structure generated by the crossover can be cleaved under acidic conditions (Scheme 5, upper); hence, the products of pMeSt and MECH copolymerization were subjected to acidolysis after purification by preparative GPC. After the reaction using trifluoroacetic acid³⁰ in dichloromethane, the MWD curves shifted to a lower MW region (Figure 1B and 1C).³¹ A pMeSt homopolymer most likely did not exist in the original product because residual shoulder peaks were not observed at a high-MW region after acidolysis. In addition, the acetal moieties derived from the isomerization of the MECH-derived propagating carbocations were also cleaved by acidolysis (Scheme 5, lower). However, the decrease in the MW after acidolysis is mainly due to the cleavage of the *sec*-benzylic ether structures derived from the crossover because fewer than one acetal unit was present per chain, as discussed in the next section. A broad peak assigned to the methine proton adjacent to the trifluoroacetoxy group was observed at 5.2–5.6 ppm in the ^1H NMR spectrum (Figure 2B). Moreover, in the ^{13}C NMR spectra, peaks assigned to the *sec*-benzylic ether structure generated by the crossover in the original copolymer disappeared upon acidolysis, and instead, new peaks assignable to the methine carbon adjacent to the trifluoroacetoxy group appeared at 78–80 ppm (Figure 3B). Importantly, the disappearance of the peaks and appearance of new peaks in similar regions were also observed in ^1H and ^{13}C NMR analysis of the product obtained by acidolysis of poly(pMeSt) with a 2-methoxyethoxy end group (Figure 3C and 3D). ^{19}F NMR analysis of the acidolysis products also confirmed the generation of structures with a trifluoroacetoxy group (Figure S13). A similar result was obtained by acidolysis of the product of

pMOS and EHMGE copolymerization (Figures 1A, S3, and S4).



Scheme 5. Cleavages of the *sec*-benzylic ether structure derived from the crossover from pMeSt to MECH and the acetal moiety by acidolysis with trifluoroacetic acid.

Discussion of the Copolymerization Mechanisms and the Structures of the Copolymers

From the results obtained above, we can determine the copolymerization mechanism and the structures of the obtained products. In the copolymerization, homopropagation reactions of both the St derivatives and the oxiranes proceeded preferentially compared to the crossover reactions, which was demonstrated by both the smaller peaks of the crossover-derived structures relative to the peaks of the main chains in NMR spectra and the approximately half to one-third decrease in the MWs after acidolysis. To estimate the preference for homopropagation over crossover reactions more accurately, we tried to determine the monomer reactivity ratios in the copolymerization of pMeSt and MECH. The copolymer composition plots are shown in Figure 4. The plots fit an S-shaped curve, indicating that homopropagation reactions occur preferentially over crossover reactions. The monomer reactivity ratios of pMeSt and MECH were tentatively estimated to be 11 and 15, respectively, by the Kelen–Tüdös method^{32,33} (these values likely hold nonnegligible experimental errors because slight differences in the compositions of the monomer units in the product significantly affect the results when the monomer reactivity ratios are much larger than one).

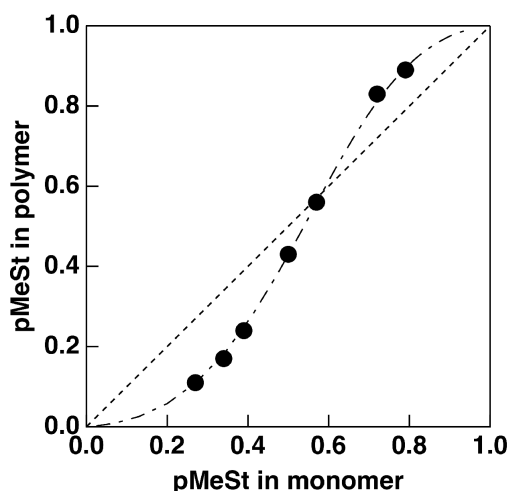


Figure 4. Copolymer compositions for the cationic copolymerization of pMeSt and MECH. The dashed-dotted line was drawn using the r values ($r_{\text{pMeSt}} = 11$, $r_{\text{MECH}} = 15$) obtained by the Kelen–Tüdös method (Figure S19). The polymerization data shown in Table S1 were used. The broken line is an azeotropic line.

An average structure of the copolymers of pMeSt and MECH was deduced from the peak area ratios in the ^1H NMR spectra and the M_n values determined by GPC analysis using a light-scattering detector. The two products listed in Table 1 (entries 5 and 6) were analyzed as summarized in Table 3. The $M_n(\text{GPC})$ values determined with a light-scattering detector were larger than the values determined with polystyrene calibration. The M_n values calculated from the area ratios of the peaks assignable to the main chain and the detectable ω -end structures (the *endo*- and *exo*-olefins and the Friedel–Crafts reaction-derived structures) were 1.3–1.4 times higher than the $M_n(\text{GPC})$ values determined with a light-scattering detector. Therefore, a small amount of undetectable ω -ends, such as a structure derived from β -proton elimination at the pMeSt-derived end or a structure resulting from reactions with impurities such as adventitious water, may exist in ^1H NMR spectra. Acetal moieties derived from the isomerization of the MECH-derived carbocation were estimated to be less than one per chain³⁴ from the peak area ratio of the acetal moieties in the ^1H NMR spectrum and the $M_n(\text{GPC})$ determined with a light-scattering detector. From these values and the results of acidolysis [$M_n(\text{GPC})$ with a light-scattering detector after acidolysis was 2.9×10^3 (entry 5)], the average structure of the copolymer is considered to be a multiblock structure consisting of 3–5 blocks in a chain, as shown in Figure 5 (see Figure S20 for the detail).

Table 3. Characterization of the Products Obtained by the Copolymerization of pMeSt and MECH^a

sample (in Table 1)	pMeSt/MECH ratio in product (mol%) ^b	detectable ω -ends (total: 1.00) ^b		Friedel- Crafts to pMeSt monomer (peaks 30, 33, etc.)	M_n (NMR) [calculated from peak areas of main chain and ω -ends]	M_n (GPC) [polystyrene calibration]	M_n (GPC) [light-scatt ering detector]	acetal units per chain ^c
		<i>endo</i> -olefin (peaks 23 and 23')	<i>exo</i> -olefin (peak 24)					
entry 5	61/39	0.20	0.40	0.40	11.2×10^3	6.4×10^3	8.2×10^3	0.49
entry 6	34/66	0.25	0.44	0.31	6.9×10^3	4.1×10^3	4.9×10^3	0.85

^a The products were analyzed after purification by preparative GPC. ^b By ¹H NMR. ^c Estimated from the absolute M_n by GPC with a light-scattering detector and the area ratio of acetal protons in the ¹H NMR spectrum.

Main components: 3–5 blocks in a chain

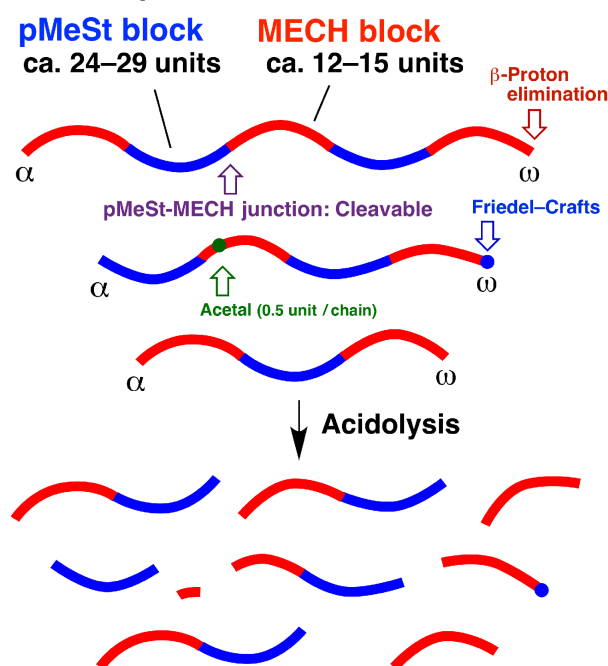


Figure 5. An average structure of the copolymer obtained by the copolymerization of pMeSt and MECH (entry 5 in Tables 1 and 3). See Figure S20 for the detail.

The reaction course of the copolymerization may be as follows. The polymerization is initiated by the trityl cation derived from $\text{Ph}_3\text{CB}(\text{C}_6\text{F}_5)_4$ or a proton generated from the initiator and adventitious water. The homopropagation reactions of pMeSt and MECH proceed preferentially, while the crossover reactions occur occasionally (Scheme 4A and 4B). The MECH-derived carbocation

sometimes isomerizes via a hydride shift, which is followed by the reaction with a MECH monomer, resulting in acetal formation (Scheme 4C), or by the reaction with a pMeSt monomer (Scheme 4B, lower). After the formation of several blocks via preferential homopropagation and occasional crossover reactions, as chain transfer reactions, β -proton elimination and/or Friedel–Crafts reactions occur at the MECH-derived propagating end to generate a dead chain and a proton (Scheme 4D). Such side reactions occur almost exclusively at oxirane-derived propagating ends. Subsequently, a new propagating chain is generated from the generated proton. Indeed, peaks assignable to the hydroxy protons at the α -ends derived from MECH were observed at 2.8–3.0 ppm in the ^1H NMR spectra (the assignments are based on the disappearance of the peaks in the presence of D_2O ; Figure 2C). The appropriate reactivity balance of the St derivative and the oxirane is of great importance for the formation of copolymers via the simultaneous consumption of both monomers through these mechanisms (Figure 6).

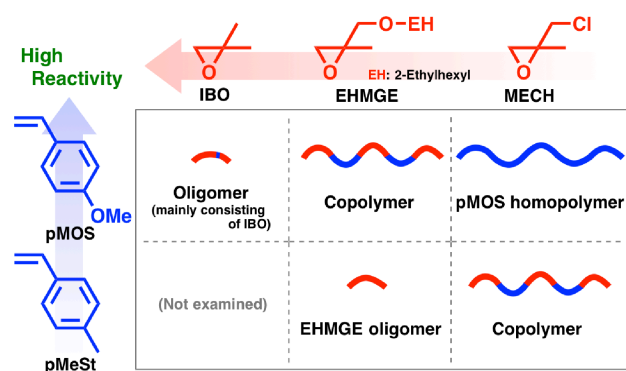


Figure 6. Major components in the products obtained by the copolymerization of styrene derivatives and oxiranes.

The possibility of the formation of the *sec*-benzylic ether structure via the reaction of the pMeSt-derived carbocation with a hydroxy group at the chain end of a MECH oligomer was eliminated by the result of the polymerization of pMeSt in the presence of an MECH homopolymer (Figure S21). The MECH polymer remained intact after the polymerization of pMeSt, which also indicates that the pMeSt-derived carbocation did not cleave the acetal moieties. In addition, the *sec*-benzylic ether structure was not likely cleaved by some acidic species, such as a trityl cation and a proton, with a $\text{B}(\text{C}_6\text{F}_5)_4^-$ counteranion during copolymerization, which was suggested by the result of the reaction of a

pMeSt–MECH copolymer with $\text{Ph}_3\text{CB}(\text{C}_6\text{F}_5)_4$ (Figure S22).

Friedel–Crafts Reactions on the Aryl Ring of the Styrene Derivatives

Friedel–Crafts reactions appeared to occur mainly between the oxirane-derived carbocation and a St derivative monomer. When we conducted the homopolymerization of MECH in the presence of a pMeSt homopolymer, the Friedel–Crafts reaction with the side chains of poly(pMeSt) did not occur (Figure S23). In addition, structures derived from the Friedel–Crafts reaction of a St derivative-derived carbocation with the aromatic ring in an intermolecular or intramolecular manner,^{35–39} which would generate a methine adjacent to two aromatic rings, were not detected in the products of pMOS and pMeSt homopolymerizations under the same conditions as those for the copolymerizations with oxiranes. These two results suggest that Friedel–Crafts reactions involving the polymer side chains and a St derivative-derived carbocation are negligible in the copolymerizations. This is in contrast to previously reported formations of star-shaped polymers and hyperbranched polymers via Friedel–Crafts reactions of a St-derived carbocation with the side chains of polystyrene.^{40,41} It is unclear whether a vinyl group-containing polymer chain resulting from the Friedel–Crafts reaction with a St derivative monomer reacted as a macromonomer in the copolymerization. However, even when such reactions occur, they occur very infrequently when considering the steric hindrance and the number of such chains.

The regioselectivity of the Friedel–Crafts reaction on the pMeSt monomer was deduced from the ^1H NMR chemical shifts of *o*, *m*, and *p*-*tert*-butylstyrenes,^{42–44} which have structures similar to the products generated by this Friedel–Craft reaction. Among the three isomers, the peaks of the vinyl protons of the *o*-isomer are shifted relative to those of the *m*- and *p*-isomers (Chart S1), likely due to the bulkiness of the *t*-butyl group.⁴⁵ The chemical shifts of the major vinyl protons in the copolymerization products (7.24, 5.41, and 5.26 ppm; peaks 28–30 in Figures 2A and 7A) were most similar to those of the *o*-isomer, while the minor vinyl protons (6.73, 5.70, and 5.19 ppm; peaks 31–33) had values similar to the other isomers (the correlations among the vinyl protons were confirmed by 2D NMR; Figures S8–S11). Therefore, the electron-donating resonance effect of the vinyl group most likely contributed more heavily to the activation of the aryl ring than the electron-donating effect of the methyl group, resulting in the Friedel–Crafts reaction preferentially occurring at the *o*-position of the vinyl group of a pMeSt monomer.

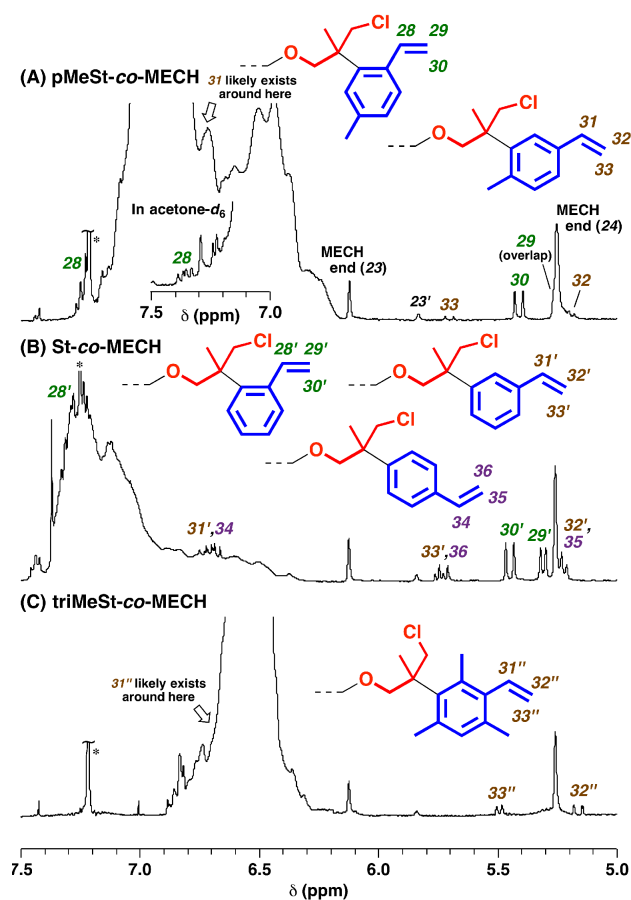
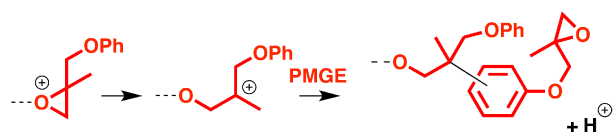


Figure 7. ^1H NMR spectra (for B, C, see Figure S25 for the spectra with a wider region) of the copolymerization product of (A) pMeSt and MECH (entry 6 in Table 1; the same spectrum as that shown in Figure 2A; see Figure S8 for the ^1H – ^1H COSY spectrum); (B) St and MECH (entry 9; see Figure S26 for the ^1H – ^1H COSY spectrum); and (C) triMeSt and MECH (entry 8). * CHCl_3 .

The occurrence of Friedel–Crafts reactions between the oxirane-derived carbocation and an aromatic ring was also confirmed in the reaction in toluene and in the copolymerization using St or a phenoxy group-containing oxirane. The copolymerization of pMeSt and MECH in toluene (entry 7 in Table 1) instead of dichloromethane resulted in a product with a very low MW (0.5×10^3). Friedel–Craft reactions with toluene appeared to occur very frequently (Figure S24). In the copolymerization of St and MECH (entry 9), Friedel–Crafts reactions occurred at any position (*o*-, *m*-, and *p*-positions) relative to the vinyl group of a St monomer (Figure 7B; see Figure S26 for the ^1H – ^1H COSY spectrum). Interestingly, the reaction preferentially occurred at the *o*-position than at the *p*-position, as confirmed

by the large area ratios of peak 30' to peaks 33' and 36, which was unexpected considering the steric repulsion. When PMGE, a β MGE derivative with a phenoxy group, was used instead of MECH (entry 10), the Friedel–Crafts reaction occurred on both the pMeSt monomer and the phenoxy group (Scheme 6; see Figures S27–S31 for details). The phenoxy group probably exhibits high reactivity due to the electron-donating effect of the alkoxy group, as exemplified by the efficient end functionalization of polyisobutylene chains by alkoxybenzenes.⁴⁶



Scheme 6. Friedel–Crafts reaction to the phenoxy group of PMGE. Intramolecular Friedel–Crafts reaction may also occur.

To suppress the Friedel–Crafts reaction to the St derivative monomer, we used triMeSt in the copolymerization with MECH (entry 8 in Table 1) because the steric hindrance of the three methyl groups on the aromatic ring was expected to disfavor the reaction between the carbocation and the ring. However, the Friedel–Crafts reaction occurred at the *m*-position of the vinyl group (Figure 7C). In addition, the copolymerization resulted in a lower MW product and less frequent crossover reactions, as determined from the result of acidolysis, compared to the copolymerization of pMeSt and MECH (Figure 1D). The methyl substituents on the ring likely disturbed the propagation reactions.

Conclusion

In conclusion, the cationic copolymerization of St derivatives and oxiranes successfully proceeded via crossover reactions when monomers with appropriate reactivities were employed. The homopropagation reactions of the two monomers preferentially occurred compared to the crossover reactions, which resulted in multiblock copolymers with several blocks per chain. The occurrence of occasional crossover reactions between the different types of monomers was confirmed by detailed analyses of the products by a series of NMR measurements and acidolysis. In particular, the comparison of the NMR spectra of the copolymerization product and a model pMeSt polymer with an

alkoxy group at the chain end before and after acidolysis contributed significantly to the assignment of the structure derived from the crossover from a St derivative to an oxirane. The results obtained in this study will contribute to both the development of novel copolymerization reactions of different types of monomers and the production of copolymer materials consisting of typically incompatible functional monomers.

Associated Content

Supporting Information

MWD curves and NMR spectra of polymerization products and polymerization data for the determination of monomer reactivity ratios.

Corresponding Authors

E-mail: kanazawaal1@chem.sci.osaka-u.ac.jp (A.K.)

E-mail: aoshima@chem.sci.osaka-u.ac.jp (S.A.)

Notes

The authors declare no competing financial interest.

Acknowledgments

We thank ADEKA Corporation (Mr. Ryo Ogawa, Dr. Kazuhide Morino, and Dr. Ken-ichi Tamaso) for kindly supplying MECH, EHMGE, and PMGE. This work was partially supported by JSPS KAKENHI Grant 18K05217.

References

1. Mecerreyes, D.; Moineau, G.; Dubois, P.; Jérôme, R.; Hedrick, J. L.; Hawker, C. J.; Malmström, E. E.; Trollsas, M. Simultaneous Dual Living Polymerizations: A Novel One-Step Approach to Block and Graft Copolymers. *Angew. Chem. Int. Ed.* **1998**, *37*, 1274–1276.
2. Puts, R. D.; Sogah, D. Y. Universal Multifunctional Initiator Containing Orthogonal Reactive Sites. Synthesis of Macromonomers and Comb Polymers Using Consecutive Controlled Free

- Radical and Cationic Ring-Opening Polymerizations. *Macromolecule* **1997**, *30*, 7050–7055.
3. Bielawski, C. W.; Louie, J.; Grubbs, R. H. Tandem Catalysis: Three Mechanistically Distinct Reactions from a Single Ruthenium Complex. *J. Am. Chem. Soc.* **2000**, *122*, 12872–12873.
 4. Bernaerts, K. V.; Du Prez, F. E. Dual/Heterofunctional Initiators for the Combination of Mechanistically Distinct Polymerization Techniques. *Prog. Polym. Sci.* **2006**, *31*, 671–722.
 5. Aoshima, H.; Uchiyama, M.; Satoh, K.; Kamigaito, M. Interconvertible Living Radical and Cationic Polymerization through Reversible Activation of Dormant Species with Dual Activity. *Angew. Chem., Int. Ed.* **2014**, *53*, 10932–10936.
 6. Satoh, K.; Hashimoto, H.; Kumagai, S.; Aoshima, H.; Uchiyama, M.; Ishibashi, R.; Fujiki, Y.; Kamigaito, M. One-Shot Controlled/Living Copolymerization for Various Comonomer Sequence Distributions via Dual Radical and Cationic Active Species from RAFT Terminals. *Polym. Chem.* **2017**, *8*, 5002–5011.
 7. Saegusa, T. Spontaneous Alternating Copolymerization via Zwitterion Intermediates. *Angew. Chem., Int. Ed. Engl.* **1977**, *16*, 826–835.
 8. Okada, M.; Yamashita, Y.; Ishii, Y. Cationic Copolymerization of 1,3-Dioxolane with Styrene. *Makromol. Chem.* **1966**, *94*, 181–193.
 9. Okada, M.; Yamashita, Y. Cationic Copolymerization of Cyclic Formals and Vinyl Ethers. *Makromol. Chem.* **1969**, *126*, 266–275.
 10. Simionescu, C. I.; Grigoras, M.; Bicu, E.; Onofrei, G. Spontaneous Copolymerization of 2-Methyl-2-oxazoline and *N*-Phenyl Maleimide. *Polym. Bull.* **1985**, *14*, 79–83.
 11. Rivas, B. L.; Pizarro, C.; Canessa, G. S. Copolymerization via Zwitterion 11. *N*-Phenylmaleimide with 2-Ethyl-2-oxazoline. *Polym. Bull.* **1988**, *19*, 123–128.
 12. Hagiwara, T.; Takeda, M.; Hamana, H.; Narita, T. Copolymerization of *N*-Phenylmaleimide and Propylene Oxide Initiated with Organozinc Compounds. *Macromolecules* **1989**, *22*, 2025–2026.
 13. Yang, H.; Xu, J.; Pispas, S.; Zhang, G. Hybrid Copolymerization of ϵ -Caprolactone and Methyl Methacrylate. *Macromolecules* **2012**, *45*, 3312–3317.
 14. Kanazawa, A.; Kanaoka, S.; Aoshima, S. Concurrent Cationic Vinyl-Addition and Ring-Opening Copolymerization Using $B(C_6F_5)_3$ as a Catalyst: Copolymerization of Vinyl Ethers and Isobutylene Oxide via Crossover Propagation Reactions. *J. Am. Chem. Soc.* **2013**, *135*, 9330–9333.

15. Kanazawa, A.; Kanaoka, S.; Aoshima, S. Rational Design of Oxirane Monomers for Efficient Crossover Reactions in Concurrent Cationic Vinyl-Addition and Ring-Opening Copolymerization with Vinyl Ethers. *Macromolecules* **2014**, *47*, 6635–6644.
16. Miyamae, Y.; Kanazawa, A.; Tamaso, K.; Morino, K.; Ogawa, R.; Aoshima, S. The Influence of the Substituents of Oxiranes on Copolymerization with Vinyl Ethers via Concurrent Cationic Vinyl-Addition and Ring-Opening Mechanisms. *Polym. Chem.* **2018**, *9*, 404–413.
17. Higuchi, M.; Kanazawa, A.; Aoshima, S. Concurrent Cationic Vinyl-Addition and Coordination Ring-Opening Copolymerization via Orthogonal Propagation and Transient Merging at the Propagating Chain End. *ACS Macro Lett.* **2017**, *6*, 365–369.
18. Hashimoto, T.; Sawamoto, M.; Higashimura, T. Selective Vinyl Cationic Polymerization of Monomers with Two Cationically Polymerizable Groups. II. *p*-Vinylphenyl Glycidyl Ether: An Epoxy-Functionalized Styrene. *J. Polym. Sci., Part A: Polym. Chem.* **1987**, *25*, 2827–2838.
19. Sawamoto, M.; Takeuchi, E.; Hashimoto, T.; Higashimura, T. Selective Vinyl Cationic Polymerization of Monomers with Two Cationically Polymerizable Groups. III. 2-Vinyloxyethyl Glycidyl Ether: An Epoxy-Functionalized Vinyl Ether. *J. Polym. Sci., Part A: Polym. Chem.* **1987**, *25*, 2717–2727.
20. Aoki, S.; Fujisawa, K.; Otsu, T.; Imoto, M. The Copolymerization of the Vinyl Monomer with a Cyclic Compounds. III. The Cationic Copolymerization of Styrene with Substituted Ethylene Oxides. *Bull. Chem. Soc. Jpn.* **1966**, *39*, 729–733.
21. Minoura, Y.; Mitoh, M. Cationic Copolymerization of Cyclic Ethers with Vinyl Compounds. III. Polymerization of Styrene in the Presence of Polyepichlorohydrin. *Makromol. Chem.* **1969**, *126*, 56–65.
22. Kim, K.; Seo, M. G.; Jung, J.; Ahn, J.; Chang, T.; Jeon, H. B.; Paik, H.-J. Direct Introduction of Hydroxyl Groups in Polystyrene Chain Ends Prepared by Atom-Transfer Radical Polymerization. *Polym. J.* **2020**, *52*, 57–64.
23. Ishihama, Y.; Sawamoto, M.; Higashimura, T. Living Cationic Polymerization of Styrene by the Methanesulfonic Acid/Tin Tetrachloride Initiating System in the Presence of Tetra-*n*-butylammonium Chloride. *Polym. Bull.* **1990**, *23*, 361–366.
24. The ratio of MECH units in the higher-MW fraction obtained from preparative GPC was lower than the original product, which suggests that oligomers mainly consisting of MECH might be

generated, although the difference of the ratios is much smaller than the case of pMOS and EHMGE (vide supra).

25. Katritzky, A. R.; Marquet, J.; Lloyd, J. M.; Keay, J. G. Kinetics and Mechanisms of Nucleophilic Displacements with Heterocycles as Leaving Groups. Part 10. Reactions of s-Alkyl Primary Amines with Pyryliums. *J. Chem. Soc., Perkin Trans. 2* **1983**, 1435–1441.
26. Zhang, X.; Corma, A. Effective Au(III)–CuCl₂-Catalyzed Addition of Alcohols to Alkenes. *Chem. Commun.* **2007**, 3080–3082.
27. Shah, S. T. A.; Singh, S.; Guiry, P. J. A Novel, Chemoselective and Efficient Microwave-Assisted Deprotection of Silyl Ethers with Selectfluor. *J. Org. Chem.* **2009**, *74*, 2179–2182.
28. Sakamoto, R.; Inada, T.; Selvakumar, S.; Moteki, S. A.; Maruoka, K. Efficient Photolytic C–H Bond Functionalization of Alkylbenzene with Hypervalent Iodine(III) Reagent. *Chem. Commun.* **2016**, *52*, 3758–3761.
29. Kiyokawa, K.; Yasuda, M.; Baba, A. Cyclopropylmethylation of Benzylic and Allylic Chlorides with Cyclopropylmethylstannane Catalyzed by Gallium or Indium Halide. *Org. Lett.* **2010**, *12*, 1520–1523.
30. Marsh, Jr. J. P.; Goodman, L. Removal of O-Benzyl Blocking Groups with Trifluoroacetic Acid. *J. Org. Chem.* **1965**, *30*, 2491–2492.
31. First, acidolysis was conducted using hydrochloric acid in 1,2-dimethoxyethane, which are similar conditions to those for the acetal cleavage of copolymers of VEs and oxiranes. However, the polymer was not degraded. Low solubility of the polymer under those conditions may be responsible for the inertness.
32. Kelen, T.; Tüdös, F. A New Improved Linear Graphical Method for Determining Copolymerization Reactivity Ratios. *React. Kinet. Catal. Lett.* **1974**, *1*, 487–492.
33. Kennedy, J. P.; Kelen, T.; Tüdös, F. Analysis of the Linear Methods for Determining Copolymerization Reactivity Ratios. II. A Critical Reexamination of Cationic Monomer Reactivity Ratios. *J. Polym. Sci., Polym. Chem. Ed.* **1975**, *13*, 2277–2289.
34. The probability of acetal formation in the copolymerization of pMeSt and MECH is lower than that in the MECH homopolymerization. An acetal moiety is always generated after the isomerization in the homopolymerization (Scheme 4C), whereas an acetal moiety is not always generated after the isomerization in the copolymerization because the carbocation reacts with not

only an MECH monomer but also a pMeSt monomer (Scheme 4B).

35. Hiza, M.; Hasegawa, H.; Higashimura, T. Cationic Oligomerization of Chlorostyrenes and *p*-Methoxystyrene: Selective Dimerization of Styrene Derivatives by Oxo Acids. *Polym. J.* **1980**, *12*, 379–385.
36. Chang, V. S. C.; Kennedy, J. P.; Ivan, B. New Telechelic Polymers and Sequential Copolymers by Polyfunctional Initiator-Transfer Agents (Inifers) 8. The Effects of Polymerization Conditions on the Functionality of Telechelic Polyisobutylenes. *Polym. Bull.* **1980**, *3*, 339–346.
37. Kennedy, J. P.; Maréchal, E. *Carbocationic Polymerization*; Wiley-Interscience, 1982; chapter 4.
38. Kennedy, J. P.; Ivan, B. *Designed Polymers by Carbocationic Macromolecular Engineering: Theory and Practice*, Hanser Publishers, Munich, New York, 1992.
39. Verebélyi, K.; Iván, B. Cationic Polymerization of Styrene by the $\text{TiCl}_4/\text{N,N,N',N'}$ -Tetramethylethylenediamin (TMEDA) Catalyst System in Benzotrifluoride, an Environmentally Benign Solvent, at Room Temperature. *Polymer* **2012**, *53*, 3426–3431.
40. Kali, G.; Szesztay, M.; Bodor, A.; Iván, B. A New Synthetic Method for the Preparation of Star-Shaped Polyisobutylene with Hyperbranched Polystyrene Core. *Macromol. Chem. Phys.* **2007**, *208*, 1388–1393.
41. Kali, G.; Szesztay, M.; Bodor, A.; Iván, B. Star and Hyperbranched Polyisobutylenes via Terminally Reactive Polyisobutylene-Polystyrene Block Copolymers. *Macromol. Symp.* **2013**, *323*, 37–41.
42. Varela, J. A.; Peña, D.; Goldfuss, B.; Denisenko, D.; Kulhanek, J.; Polborn, K.; Knochel, P. Diastereoselective Remote C–H Activation by Hydroboration. *Chem. Eur. J.* **2004**, *10*, 4252–4264.
43. Gao, Y.; Ou, Y.; Gooßen, L. J. Pd-Catalyzed Synthesis of Vinyl Arenes from Aryl Halides and Acrylic Acid. *Chem. Eur. J.* **2019**, *25*, 8709–8712.
44. Su, W.; Urgaonkar, S.; McLaughlin, P. A.; Verkade, J. G. Highly Active Palladium Catalysts Supported by Bulky Proazaphosphatane Ligands for Stille Cross-Coupling: Coupling of Aryl and Vinyl Chlorides, Room Temperature Coupling of Aryl Bromides, Coupling of Aryl Triflates, and Synthesis of Sterically Hindered Biaryls. *J. Am. Chem. Soc.* **2004**, *126*, 16433–16439.
45. Akermarck, B.; Ljungqvist, A. The Thermal Formation of Bialkyls from Alkylmetals. III. Thermolysis of Nephyl Complexes of the First Row Transition Metals. *J. Organomet. Chem.* **1979**,

182, 47–58.

46. Morgan, D. L.; Martinez-Castro, N.; Storey, R. F. End-Quenching of TiCl_4 -Catalyzed Quasiliving Polyisobutylene with Alkoxybenzenes for Direct Chain End Functionalization. *Macromolecules* **2010**, *43*, 8724–8740.